

## A 2-60 GHz Microwave and Millimeter-Wave Planar Antenna with Simple Structure

Aliakbar Dastranj\*

[Corresponding Author] Electrical Engineering Department;  
Faculty of Engineering; Yasouj University; Yasouj, Iran;  
Email: dastranj@yu.ac.ir

Saman Heidari

Department of Electrical and Electronics Engineering;  
Shiraz University of Technology; Shiraz, Iran;  
Email: Sa.Heidari@sutech.ac.ir

Received: 04 Apr. 2022

Revised: 12 May 2022

Accepted: 25 Jun. 2022

**Abstract:** This paper presents a compact planar microstrip-fed quasi-fractal antenna for 2-60 GHz microwave and millimeter-wave systems. The ultra-wideband property of the antenna is obtained by accomplished two iterations of Sierpinski circular slots on the circular radiator along with using curve-shaped ground plane. The overall antenna size is  $28 \times 28 \times 1.6 \text{ mm}^3$  which is printed on FR4 substrate with a dielectric constant of 4.4. The designed antenna with a simple and compact structure provides 187% (reflection coefficient less than  $-10\text{dB}$ ) impedance bandwidth, which can cover S (2-4 GHz), C (4-8 GHz), X (8-12 GHz), Ku (12-18 GHz), K (18-26 GHz), Ka (26-40 GHz), and U (40-60 GHz) frequency bands. Due to small electrical dimension of the designed antenna ( $0.187 \lambda \times 0.187 \lambda$ ), a large bandwidth dimension ratio of 5347 is resulted. The numerical outcomes are verified by experimental measurements. Measured data are in good agreement with the simulated results. The frequency- and time-domain characteristics of the antenna including impedance matching, far-field patterns, gain, and group delay are presented and discussed. Results show that the antenna is an excellent radiating component for use in several military and industrial systems.

**Index Terms:** Compact Size, Equivalent Circuit Model, Microstrip-fed, Microwave, Millimeter Wave, Sierpinski Circular Slots.

## I. INTRODUCTION

A fractal antenna can be designed to operate over a wide range of frequencies using the self-similarity properties associated with fractal geometry structures. Printed fractal antennas can be used in variety of wideband applications, especially where space is limited. The geometry of fractal antenna was defined by Mandelbort in 1975 [1]. A fractal is a self-similar geometric shape of the whole structure

which can be subdivided into the parts; each of the part is a reduced size copy of the whole geometry of the antenna. Fractal geometry has some advantages over simple planar radiator such as: at arbitrarily minute scale it has an excellent structure, it can be easily described in traditional Euclidean geometry by using its irregular shape, simple and recursive, improving input resistance of antennas, and enhance electrical area [2]. Thus, to miniaturize the antenna size with high radiation efficiency, fractal antennas are most suitable [3].

As the demand for high data transmission is increasing, long range frequency spectrum is needed. Super-wideband (SWB) technology is generally used for having bandwidth (BW) ratio greater than 10:1 [4]. As this technology provides higher data rates and higher and more balanced BW, it can be used to send the data, voice, and video at higher speeds or ranging and monitoring applications, both in civil and military systems [5, 6].

To fulfill the broadband communication systems requirements, several investigations on fractal antennas have been reported [7]-[11]. In [7], a fractal monopole antenna with a volume of  $24 \times 24 \times 1 \text{ mm}^3$  can cover a bandwidth of 2.1–11.52 GHz. In [8], a CPW-fed octagonal Sierpinski fractal antenna can cover a bandwidth of 3.73–20 GHz. A multiband Koch-like sided fractal bow-tie dipole antenna was reported in [9]. The fractal printed bow-tie antenna in [10] can cover bandwidth from 1.64 to 1.94 GHz. In [11], an antenna with notch band characteristics that uses koch fractal for UWB applications was proposed. Different fractal antennas for wideband application were reported in [12]-[14]. In [12], a circular-hexagonal fractal antenna was investigated for many wireless communications systems such as ISM, Wi-Fi, GPS, Bluetooth, WLAN, and UWB. It was made of iterations of a hexagonal slot inside a circular metallic patch with a transmission line. A partial ground plane and asymmetrical patch toward the substrate were used for designing the antenna to achieve a wide bandwidth. In [13], a hexagonal shaped fractal antenna with triangular slot and a total size of  $20 \times 33.4 \times 1.57 \text{ mm}^3$  for wideband application was presented. In [14], a printed star-triangular fractal microstrip-fed monopole antenna with semi-elliptical ground plane was presented for wideband applications. A miniaturized UWB antenna based on Sierpinski square slots was reported in [15]. It has a compact dimension of only  $28 \times 28 \text{ mm}^2$  and a fractional bandwidth of about 127.3% (3.41-15.37 GHz). A printed Koch

Snowflake antenna with an operating frequency range of (3.4–16.4GHz for UWB radio frequency identification applications was presented in [16].

The low-profile SWB antenna with a large bandwidth dimension ratio (BDR) can be found in few papers because having compact size and an extremely large BW with stable radiation characteristic at higher frequencies is very challenging [17]. In [18], a circular shape fractal antenna with BW ratio of 7.2:1 was presented. In [19], a dual band-notched SWB coplanar waveguide (CPW)-fed antenna with electrical dimension of  $0.18 \lambda \times 0.13 \lambda$ , BW ratio of 14.28:1 and operating BW of 173.8% was proposed. In [20], the antenna has a very large electrical dimension of  $0.45 \lambda \times 0.45 \lambda$  and BW of 1.0-19.4 GHz with a very low BDR. In addition, the antenna presented in [21] has a BW ratio of 10.16:1 and electrical dimension of  $0.47 \lambda \times 0.32 \lambda$  which is large in size compared to the BW the antenna provides. A CPW-fed hexagonal Sierpinski fractal radiator for SWB applications with the electrical dimension of  $0.32 \lambda \times 0.34 \lambda$  is introduced in [22] which has a BW ratio of 11:1. In [23], a monopole antenna fed by microstrip line with a BW ratio of 13:1 and electrical dimension of  $0.17 \lambda \times 0.37 \lambda$  has been proposed which has some radiation characteristic problems. The antenna presented in [24] has a low BDR due to its large electrical dimension of  $0.35 \lambda \times 0.20 \lambda$  compare to the BW of 3-35 GHz which the antenna can provide. Also, a set of SWB antennas were presented in [25]-[31] which will be compared to the proposed structure in section 3.

In this paper, a low-profile 2-60 GHz (BW ratio of 30:1) planar quasi-fractal antenna with simple structure, electrical dimension of  $0.187 \lambda \times 0.187 \lambda$  (overall dimension of  $28 \times 28 \times 1.6 \text{ mm}^3$ ), and operating BW of 187% is presented. These goals are accomplished by using two iterations of Sierpinski circular slots on the circular radiator along with curve-shaped ground plane. To establish the optimum operation, the antenna dimensions have been optimized by full-wave Ansys Electromagnetics simulator package. The measured results of the fabricated prototype in frequency-and time-domain are also presented and compared with the simulated results. The proposed antenna has desirable performance based on the achievement results in both simulation and measurement. The performance of the designed antenna is compared with several recent SWB antennas. In spite of small electrical dimension of the antenna compare to the others, a large BDR of 5347 is provided. The results show that the antenna is an excellent choice for use in several microwave and millimeter-wave systems. The novelty of the proposed antenna lies in its simple structure, compact size, high BDR, and SWB operation. The antenna design and the process of reaching the final structure will be discussed in the following sections.

## II. DESIGN AND OPTIMIZATION OF THE ANTENNA

The geometry of the proposed SWB antenna with detailed and necessary dimensions effective on its impedance BW characteristics is shown in Fig. 1. Optimization of the dimensions has been accomplished by using Ansys Electromagnetics software package. The antenna is printed on FR4 substrate with permittivity of 4.4, loss tangent of 0.02 and thickness of 1.6mm. The copper cladding's thickness and the electrical size of the antenna are  $35\mu\text{m}$  and  $0.187\lambda \times 0.187\lambda$ , respectively. As illustrated in Fig. 1, two iterations of Sierpinski circular slots on the circular radiator along with curve-shaped ground plane is used to achieve multi-frequency resonance characteristic, and consequently SWB operation. The optimal dimensions of the proposed antenna are as follows (in mm):  $W = 28$ ,  $L = 28$ ,  $W_f = 3$ ,  $L_f = 5.96$ ,  $h = 2$ ,  $d = 8$ ,  $d_1 = 4$ ,  $r = 6$ , and  $s = 0.88$ .

To further understand the antenna performance, it is recommended to obtain its equivalent circuit model. Fig. 2 illustrates the equivalent circuit model of the designed antenna. In the antenna circuit model described in Fig. 2,  $L_f$  and  $C_f$  represent the feed inductance and the antenna static capacitance, respectively. The equivalent circuit of the circular patch is formed of resistance ( $R_p$ ), inductance ( $L_p$ ), and capacitance ( $C_p$ ). In Fig. 2, the impedance of the circular patch is modelled by a parallel RLC circuit. The fractal slots are represented by L-C resonator cells ( $L_{s1}$ - $C_{s1}$ ,  $L_{s2}$ - $C_{s2}$ ), whereas  $C_c$  represents the mutual coupling among the radiating patch and the ground plane. The partial ground plane is modelled by L-C resonator ( $L_g$ - $C_g$ ). For further understanding, the antenna wideband impedance discontinuities are introduced in the equivalent circuit and represented by parallel RLC resonators ( $R_1$ - $L_1$ - $C_1$ ,  $R_2$ - $L_2$ - $C_2$ ,  $R_3$ - $L_3$ - $C_3$ ).

In the evolution procedure of the antenna design, different structures shown in Fig.3 have been simulated by using Ansys Electromagnetics and comparison results of reflection coefficient curves are also illustrated. In the initial structure, a simple circular radiating patch with a rectangular finite ground plane has been considered. It can be observed that the initial structure exhibits  $|S_{11}| > -10$  dB over the frequency bands of 8.9-10.8, 15.65-17.6, and 21.1-24 GHz. In iteration 0, a curve-shaped ground plane is used to improve the impedance matchin of the antenna. In iteration 1, a circular slot with radius of 8 mm is etched on the central section of radiating patch. As a result, impedance matching at higher frequencies of the bandwidth is improved. In the final step, the second iteration of circular slots are etched on the radiating patch and the best result including 2-60 GHz bandwidth is achieved in iteration 2.

The current distribution on the patch and ground of different stages of antenna design (shown in Fig. 3) at frequency of 30 GHz is shown in Fig. 4. Creating a curved ground plane (Fig. 4c and d) due to gradual changes in the geometric structure, increases the bandwidth compared to the previous stage (Fig. 4a and b). The embedding of a circular gap in the patch (Fig. 4e and f) causes the formation

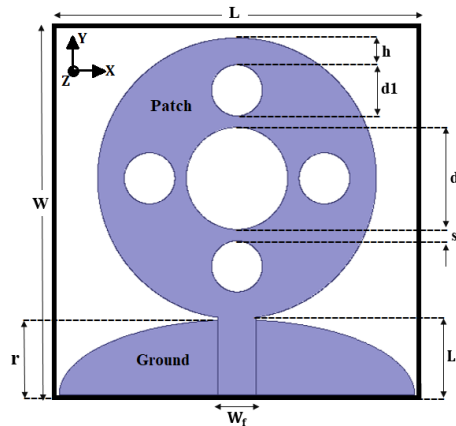


Fig. 1. Geometry of the proposed antenna with detailed dimensions

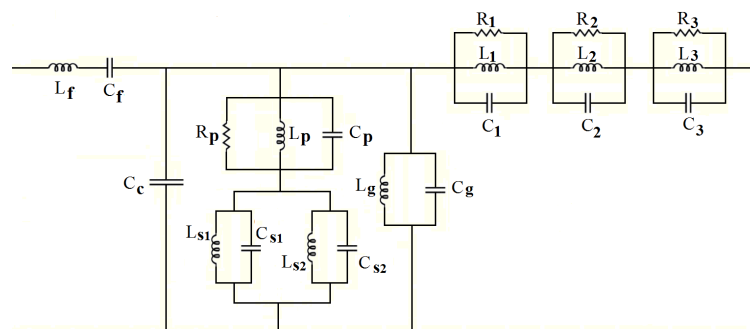


Fig. 2. Simplified equivalent circuit model of the antenna

of capacitance and also due to the increase of inductance property created caused by lengthening the path current on the patch, leading to increases the bandwidth. By creating a circular gap with a smaller radius and it repeating (Fig. 4g and h), more resonances are created in the structure, and their combination causes better impedance matching and increased bandwidth. Electric and magnetic resonances created in the antenna are considered in the equivalent circuit model of Fig. 2. Also, from Fig. 4(g and h) it can be seen that the current paths have been lengthened because of the introduction fractal on the patche which leads to an increase in electrical length and hence a decrease in overall patch size. The coupling of energy among the radiating patch and the ground plane is very low value and the antenna produces very low value of capacitance and inductance. Therefore, according to the relationship

$$f = \frac{1}{2\pi\sqrt{LC}} \quad (1)$$

the low value of capacitance and inductance produces high value of resonance frequency. Therefore, this helps in the impedance matching and very wide bandwidth.

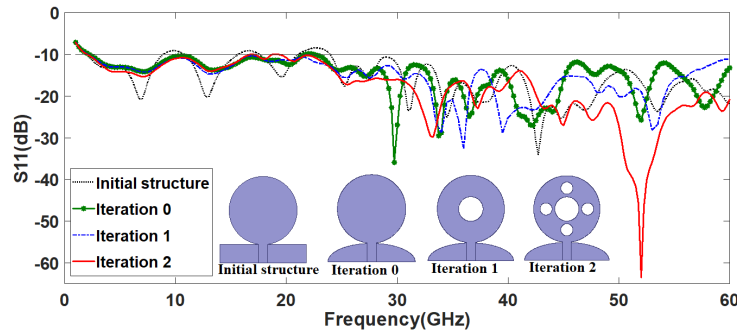


Fig. 3. Simulated reflection coefficient curves of the antenna structures

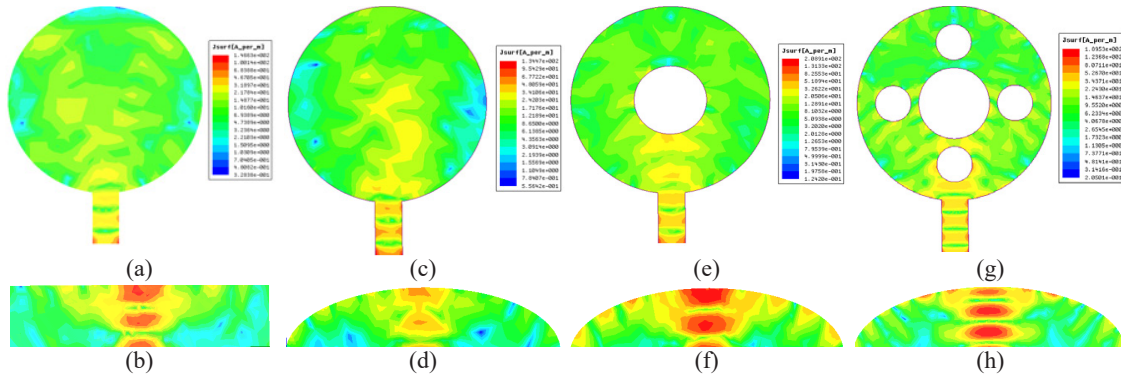


Fig. 4. Current distribution on the patch and ground of the (a) and (b) initial structure, (c) and (d) iteration 0, (e) and (f) iteration 1 and (g) and (h) iteration 2 related to Fig. 3 at 30 GHz

Fig. 5 shows the final structure of the proposed antenna and its reflection coefficient versus frequency. Numerical parametric analysis via Ansys Electromagnetics was performed to understand the influence of the antenna physical dimensions on the impedance bandwidth. It was found that maximum width of the ground plane,  $r$ , and diameter of the first circular slot on the radiator,  $d$ , have considerable influence on the SWB performance of the proposed antenna. As depicted in Fig. 6, the maximum width of the ground plane  $r$  affects the antenna reflection coefficient over the entire SWB spectrum. It is seen that the resonance frequencies of the antenna at 6, 20, 30, 33, 38, and 52 GHz are largely depend on  $r$ . The effects of diameter  $d$  is presented in Fig. 7 while other geometrical parameters are kept fixed. It can be observed that this parameter influences the reflection coefficient at frequencies higher than 20 GHz. Results of Figs. 6 and 7 show that selecting the optimal values of  $r=6$  mm and  $d=8$  mm leads to maximum impedance bandwidth.

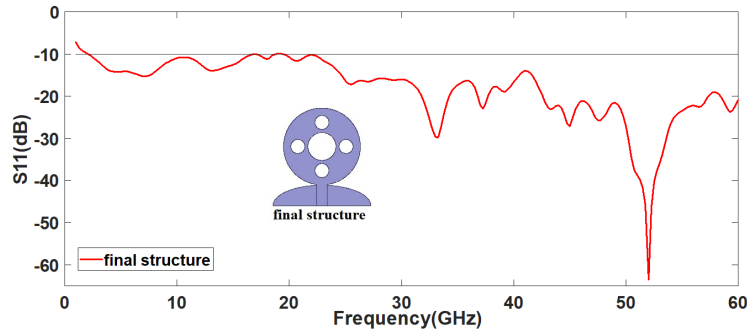


Fig. 5. Final structure of the proposed antenna and its reflection coefficient curve

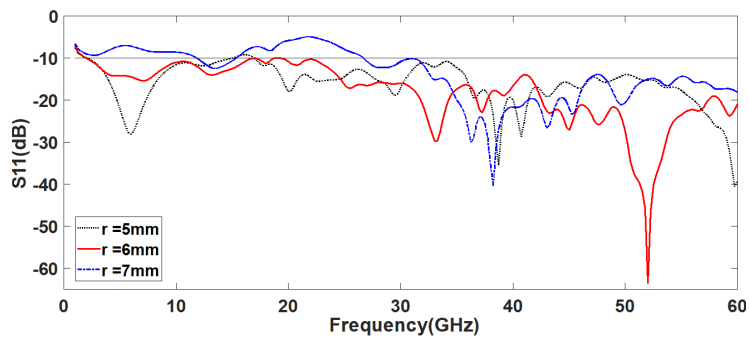


Fig. 6. Reflection coefficients for different values of r

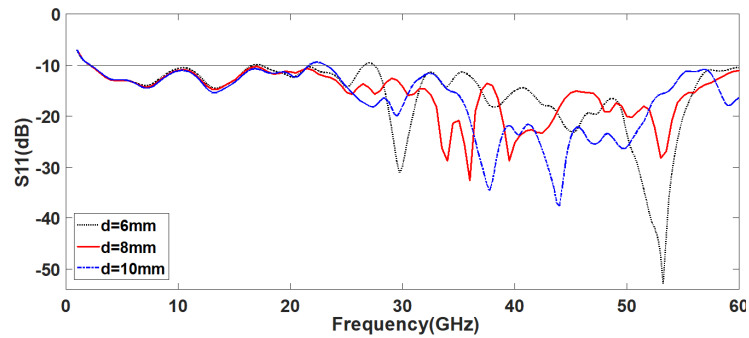


Fig. 7. Reflection coefficients for different values of d

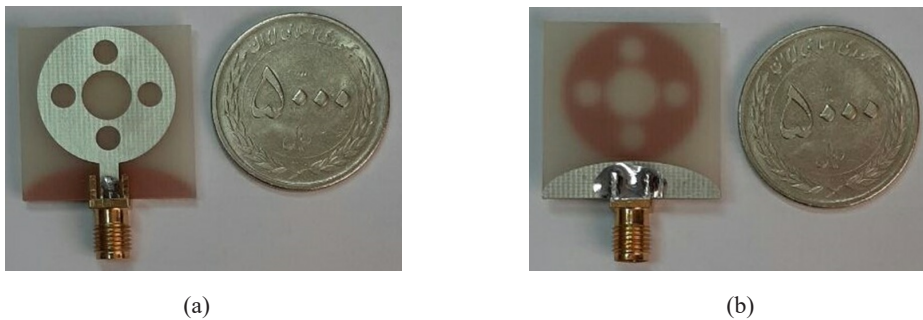


Fig. 8. Photograph of the proposed antenna prototypes. (a) Top view, (b) Bottom view

### III. EXPERIMENTAL VERIFICATION AND DISCUSSION

In order to validate the numerical results obtained by Ansys Electromagnetics, the designed quasi-fractal planar antenna was constructed and tested. Fig. 8 illustrates the photograph of the fabricated prototypes. The designed antenna is connected to a  $50\Omega$  SMA connector for signal transmission. The part number of SMA female connector is SC8026 which normally operates from DC up to a frequency of 18 GHz and offers excellent voltage standing wave ratio (VSWR) of 1.23:1. However, this connector features VSWR of about 1.45:1 for frequency range of 18-60 GHz. It is a low cost connector with reasonable loss. Fig. 9 presents the comparison of experimental and numerical reflection coefficient curves of the proposed antenna. Measured and simulated results show that the designed fractal antenna can cover a SWB frequency range, from 2 to 60 GHz (187% impedance bandwidth) including S (2-4 GHz), C (4-8 GHz), X (8-12 GHz), Ku (12-18 GHz), K (18-26 GHz), Ka (26-40 GHz), and U (40-60 GHz) frequency bands. There is a negligible difference between the experimental and numerical results due to the measurement errors, fabrication tolerances, and SMA soldering effects. In order to further understand the utility of the proposed antenna over the entire operating bandwidth, other radiation characteristics such as far-field patterns and realized gain must also be carefully investigated. The far-field radiation patterns of the antenna were measured at different frequencies over 2-40 GHz range. Due to limitation of test equipment, patterns at frequencies higher than 40 GHz were not measured. The numerical and experimental E (y-z)- and H (x-z)-plane patterns at 2, 20, and 40 GHz are compared in Fig. 10. A good concordance between the numerical and experimental outcomes is observed. As illustrated in this figure, the antenna features nearly omnidirectional patterns specifically in the x-z plane. As shown in Fig. 10 (d), pattern fluctuation at 60 GHz is considerable. Furthermore, the cross polarization level increases at higher frequencies due to excitation of higher order modes. So, the overall bandwidth of the antenna is limited by radiation pattern performance at frequency higher than 60 GHz. Fig. 11 plots the simulated and measured gain curve of the proposed antenna versus frequency. As shown in this figure, the maximum value of the measured antenna gain is 6 dBi which occurs at 35 GHz. The measured gain has an average value of 3.65 dBi. It should be noted that the antenna gain is moderate over the working band respecting the compact size and omnidirectional behavior of the antenna.

In SWB antennas, BDR is an important parameter that the higher BDR signifies wider frequency band and compactness of the proposed antenna compare to the other structures. BDR indicates how much operating bandwidth (in percentage) can be provided per electrical area unit. The equality is defined as  $BDR = BW(\%) / (\lambda_{Length} \times \lambda_{Width})$  [19] and [23]. In this equation,  $\lambda$  is the wavelength at the lower cut-off frequency of the working BW. In spite of small electrical

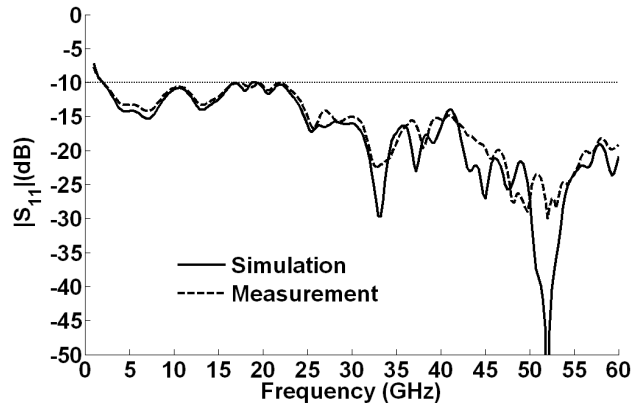
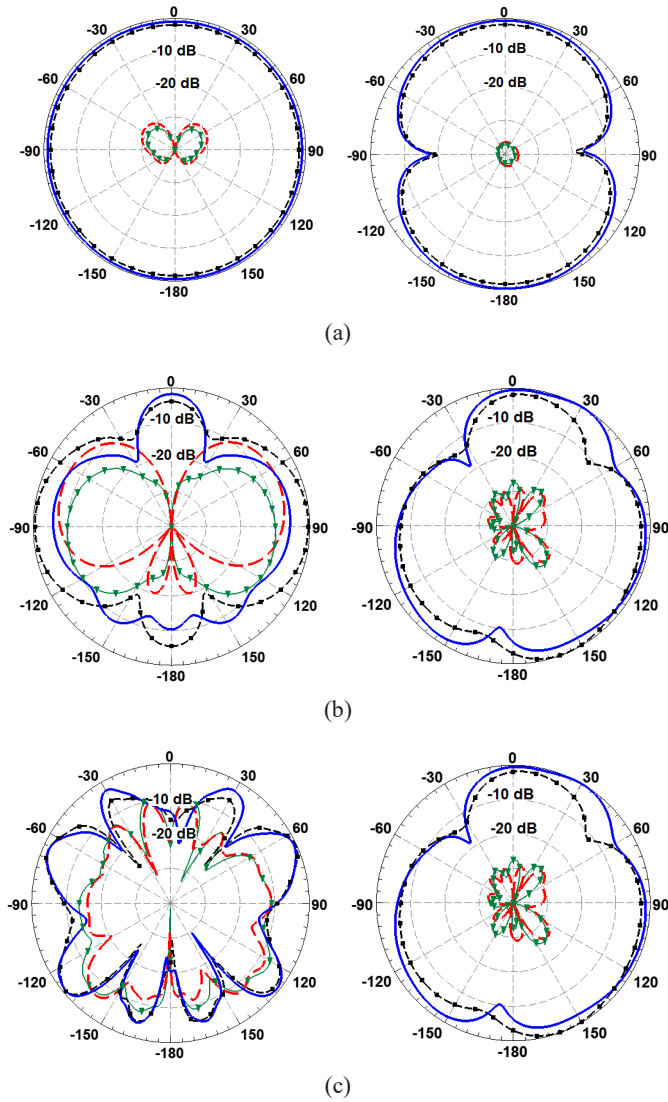


Fig. 9. Numerical and experimental reflection coefficient curves of the antenna



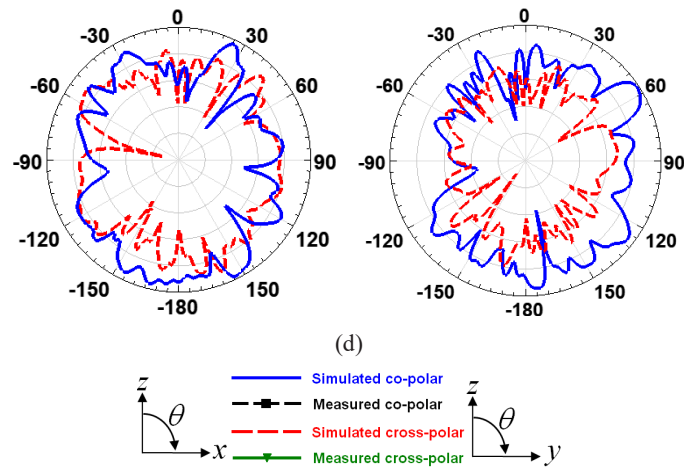


Fig. 10. E (y-z)- and H (x-z)-plane patterns of the antenna (left: x-z plane, right: y-z plane) at (a) 2 GHz, (b) 20 GHz, (c) 40 and (d) 60 GHz

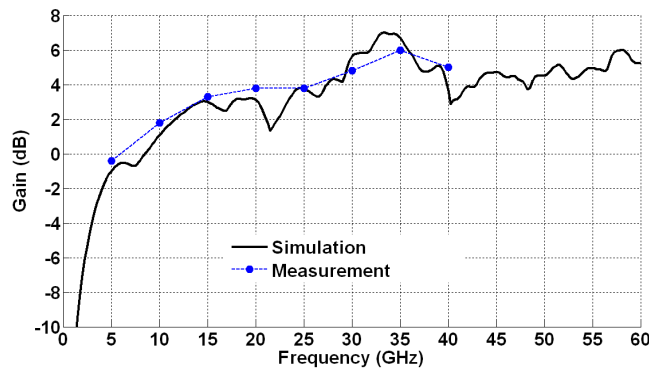


Fig. 11. Antenna gain curves versus frequency

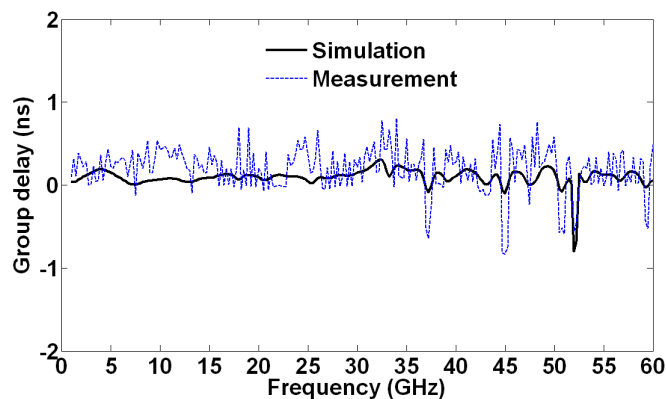


Fig.12. Group delay of the proposed antenna

dimension of the proposed antenna and wide impedance bandwidth, a large BDR of 5347 is exhibited. Accordingly, it can be concluded that the proposed SWB antenna can provide good BW ratio and very larger BDR characteristics with much smaller size in comparison to the other SWB antenna structures studied in [19-31].

**Table 1. Comparison between the proposed antenna and other reported works**

Ref.	Electrical dimension	BDR	BW ratio
[20]	$0.45\lambda \times 0.45\lambda$	890.83	19.40:1
[21]	$0.47\lambda \times 0.32\lambda$	1102.91	10.16:1
[22]	$0.32\lambda \times 0.34\lambda$	1531.89	11.00:1
[23]	$0.17\lambda \times 0.37\lambda$	2735.00	13.06:1
[24]	$0.35\lambda \times 0.20\lambda$	2400.00	11.60:1
[25]	$0.23\lambda \times 0.32\lambda$	2230.00	10.31:1
[26]	$0.41\lambda \times 0.29\lambda$	1347.24	9.11:1
[27]	$0.44\lambda \times 0.44\lambda$	905.00	13.63:1
[28]	$2.00\lambda \times 2.00\lambda$	33.33	5.00:1
[29]	$0.32\lambda \times 0.34\lambda$	1682.00	25.00:1
[30]	$0.43\lambda \times 0.45\lambda$	950.77	25.00:1
[38]	$0.27\lambda \times 0.23\lambda$	2541.12	10.00:1
[39]	$0.28\lambda \times 0.40\lambda$	1702.05	41.70:1
[40]	$0.28\lambda \times 0.26\lambda$	2576.23	31.14:1
[41]	$0.23\lambda \times 0.30\lambda$	2292.75	8.60:1
Proposed	$0.187\lambda \times 0.187\lambda$	5347	30:1

Along with frequency-domain analysis, time-domain performance should also be analysed in order to be sure of the SWB operation. The time-domain analysis required two identical designed antennas, one as the transmitter and the other one as a receiver, in the adjustment of face-to-face and side-by-side. Time-domain analysis of both configurations was considered using CST Microwave Studio by a distance of 50 cm. Time taken by the antenna to receive the pulse is indicated by an important parameter named group delay. In order to provide desirable time-domain behavior in a typical SWB system, constant group delay is required over the entire working band [32-37]. Group delay of side-by-side orientation is shown in Fig. 12 which its peak-to-peak variation is less than 2 ns over the entire frequency band. Although the result of the face-to-face configuration has not been discussed in this section, similar results were obtained which indicate an acceptable time-domain performance.

Temperature humidity test chamber is able to simulate a wide range of temperature and humidity environments. It was used in testing fabricated antenna for its tolerances of heat, cold, dry and humidity. It was found that operating temperatures ranging from  $-50^{\circ}\text{C}$  to  $+70^{\circ}\text{C}$ , and humidity range is from 10% to 95% RH. These results show that the antenna can perform in environments with a wide range of operating temperatures and humidity.

The results of the comparison between the designed antenna and other SWB antenna structures studied in [20-30] and [38-41], are presented in Table 1 on the basis of BDR. In spite of small electrical dimension of the proposed antenna compare to the others, a high BDR of 5347 is exhibited. Accordingly, it can be concluded that the proposed SWB antenna can provide good BW ratio and high BDR characteristics with much smaller size in comparison to the other antennas.

#### IV. CONCLUSION

A low-profile 2-60 GHz printed microstrip-fed antenna has been presented. In order to jointly achieve compact structure with a SWB performance, two iterations of Sierpinski circular slots on the circular radiator along with curve-shaped ground plane are employed. To achieve the optimum operation, the antenna dimensions have been optimized by full-wave Ansys Electromagnetics simulator package. Moreover, to further understanding of the antenna performance, the equivalent circuit mode of the designed antenna has been studied. The antenna with electrical dimension of  $0.187 \lambda \times 0.187 \lambda$  provides BW ratio of 30:1 and operating BW of 187% including S (2-4 GHz), C (4-8 GHz), X (8-12 GHz), Ku (12-18 GHz), K (18-26 GHz), Ka (26-40 GHz), and U (40-60 GHz) frequency bands.. The novelty of the proposed antenna lies in its simple structure, compact size, high BDR, and SWB operation. The measured results of the fabricated prototype in frequency-and time-domain are also presented and compared with the simulated results. The performance of the designed antenna is compared with several recent SWB antennas. In spite of small electrical dimension of the antenna compare to the others, a large BDR of 5347 is provided. Hence, it can be concluded that the presented antenna can provide good BW ratio and very larger BDR characteristics with much smaller size in comparison to the other antennas. Based on the achievement results, the antenna can be used in military and industrial systems at microwave and millimeter-wave spectrum.

#### REFERENCES

- [1] K. Kharat, S. Dhoot and J. vajpai. "Design of compact multiband fractal antenna for WLAN and WiMAX Applications," *IEEE, International conference on pervasive computing (ICPC)*, 2015.
- [2] D. H. Werner, S. Ganguly, "An overview of Fractal Antenna Engineering Research", *IEEE Antennas and Propagation Magazine*, vol. 45, pp.38-57, 2003.
- [3] J. Gianvittorio and Y. Rahmat-Samii, "Fractal element antennas: A compilation of configurations with novel characteristics," *IEEE Antennas and Propagation Society International Symposium*, Salt Lake City, UT, USA, 16-21 July, 2000.
- [4] H. M. Bernety, B. Zakeri, R. Gholami, "Design of a novel directional microstrip-fed super-wideband antenna," *Modares Journal of Electrical Engineering*, vol. 11, no.3, pp. 2563-2570, 2011.

- [5] P. Okas, A. Sharma and R. Ku. Gangwar, "Super wideband CPW-fed modified square monopole antenna with stabilized radiation characteristics," *Microw. Opt. Technol. Lett.*, vol. 60, pp. 568–575, 2018.
- [6] D. Li and J.-F. Mao, "Sierpinski-like sided multifractal dipole antenna," *Progress In Electromagnetics Research*, vol. 130, pp. 207-224, 2012.
- [7] M. N. Moghadasi, R.A. Sadeghzadeh, T. Aribi, T. Sedghi, B.S. Virdee, "UWB monopole microstrip antenna using fractal tree unit-cells," *Microwave and optical technology letters*, vol. 54, no. 10, pp. 2366–2370, Oct. 2012.
- [8] S. Singhal, P. Singh and A. K. Singh, "Asymmetrically CPW-FED Octagonal Sierpinski UWB Fractal Antenna," *Microwave and Optical Technology letter*, vol. 58, no. 7, July 2016.
- [9] D. Li, and J.-f. Mao, "A koch-like sided fractal bow-tie dipole antenna," *IEEE Trans. Antennas Propag.*, vol. 60, no. 5, pp. 2242-2251, 2012.
- [10] Y.-W. Zhong, G.-M. Yang, and L.-R. Zhong, "Gain enhancement of bow-tie antenna using fractal wideband artificial magnetic conductor ground," *Electron. Lett.*, vol. 51, no. 4, pp. 315-317, Feb. 2015.
- [11] S. Kumar Terlapu, Ch. Jaya and G.S. Raju, "On the Notch Band Characteristics of Koch Fractal Antenna for UWB Applications," *International Journal of control theory and applications*, vol. 10, no. 6, pp. 0974-5572, 2017.
- [12] M. A. Dorostkar, M. T. Islam, and R. Azim, "Design of A Novel Super Wide Band Circular-Hexagonal Fractal Antenna," *Progress In Electromagnetics Research*, Vol. 139, 229-245, 2013.
- [13] B. L. Shahu, S. Pal, and N. Chattoraj, "Design of Super Wideband Hexagonal-Shaped Fractal Antenna With Triangular Slot," *Microwave and Optical Technology Letters*, vol. 57, no. 7, pp. 1659-1662, July 2015.
- [14] V. Waladi, N. Mohammadi, Y. Zehforoosh, A. Habashi and J. Nourinia, "A Novel Modified Star-Triangular Fractal (MSTF) Monopole Antenna for Super-Wideband Applications," *IEEE Antennas and Wireless Propagation Letters*, vol. 12, pp. 651-654, 2013.
- [15] A. Tanweer, B. K. Subhash, and C. B. Rajashekhar, "A miniaturized decagonal Sierpinski UWB fractal antenna," *Progress In Electromagnetics Research C*, vol. 84, 161-174, 2018.
- [16] H. Tizyi, F. Riouch1, A. Tribak1, A. Najid1, and A. Mediavilla, "CPW and microstrip line-fed compact fractal antenna for UWB-RFID applications," *Progress In Electromagnetics Research C*, Vol. 65, 201–209, 2016.
- [17] W. Balani, M. Sarvagya, T., MM, M. P. Ali, J. Anguera, A. Andujar, and S. Das, "Design techniques of super-wideband antenna-Existing and future prospective," *IEEE Access*, vol. 7, pp. 141241-141257, 2019.
- [18] A. Dastranj, F. Ranjbar, and M. Bornapour, "A New Compact Circular Shape Fractal Antenna for Broadband Wireless Communication Applications," *Progress In Electromagnetics Research C*, vol. 93, pp. 19-28, 2019.
- [19] A. Dastranj, G. Lari, and M. Bornapour, "A compact dual band-notched SWB antenna with high bandwidth dimension ratio," *International Journal of Microwave and Wireless Technologies*, vol. 13, pp. 87–93, 2021.
- [20] J. Yeo, and J. I. Lee, "Coupled-sectorial-loop antenna with circular sectors for super wideband applications," *Microw Opt Technol Lett.*, vol. 60, pp. 1683–1689, July 2014.
- [21] S. Hakimi, S. K. A. Rahim, M. Abedian, S. Noghabaei and M. Khalily, A.K. Singh, "CPW-fed transparent antenna for extended ultrawideband applications," *IEEE Antennas Wireless Propag. Lett.*, vol. 10, pp. 1701–1707, 2016.
- [22] S. Singhal and A. K. Singh, "CPW-fed hexagonal Sierpinski super wideband fractal antenna," *IET Microw. Antennas Propag.*, vol. 8, no. 1, pp. 39–45, 2014.
- [23] K. R. Chen, C. Sim, J. S. Row "A compact monopole antenna for super wideband applications," *IEEE Antennas Wireless Propag. Lett.*, vol. 10, pp. 488–491, 2011.
- [24] B. L. Shahu, S. Pal, N. Chattoraj "Design of super wideband hexagonal-shaped fractal antenna with triangular slot," *Microw. Opt. Technol. Lett.*, vol. 57, pp. 1659–1662, July 2015.

- [25] C. Deng, Y. J. Xie, and P. Li, "CPW-fed planar printed monopole antenna with impedance bandwidth enhanced," *IEEE Antennas Wireless Propag. Lett.*, vol. 8, pp. 1394–1397, 2009.
- [26] M. N. Srifi, S. K. Podilchak, M. Essaïdi, and Y. M. M. Antar, "Compact disc monopole antennas for current and future ultrawideband (UWB) applications," *IEEE Trans. Antennas Propag.*, vol. 59, no. 12, pp. 4470–4480, Dec. 2011.
- [27] S. Cheng, P. Hallbjörner, and A. Rydberg, "Printed slot planar inverted cone antenna for ultrawideband applications," *IEEE Antennas Wireless Propag. Lett.*, vol. 7, pp. 18–21, 2008.
- [28] A. Azari, "A new super wideband fractal microstrip antenna," *IEEE Trans. Antennas Propag.*, vol. 59, no. 5, pp. 1724–1727, May 2011.
- [29] Y. Dong, W. Hong, L. Liu, Y. Zhang, and Z. Kuai, "Performance analysis of a printed super wideband antenna," *Microw. Opt. Technol. Lett.*, vol. 51, no. 4, pp. 949–956, Apr. 2009.
- [30] J. Liu, K. P. Esselle, S. G. Hay, and S. Zhong, "Achieving ratio bandwidth of 25 : 1 from a printed antenna using a tapered semi-ring feed," *IEEE Antennas Wireless Propag. Lett.*, vol. 10, pp. 1333–1336, 2011.
- [31] S. Singhal and A. K. Singh, "CPW-fed phi-shaped monopole antenna for super wide-band applications," *Progress in Electromagnetics Research*, vol. 64, pp. 105–116, 2016.
- [32] A. Dastranj, "Low-profile ultra-wideband polarisation diversity antenna with high isolation," *IET Microwaves, Antennas Propag.*, vol. 11, no. 10, pp. 1363-1368, Aug. 2017.
- [33] A. Dastranj, "Modified end-fire bow-tie antenna fed by microstrip line for wideband communication systems," *Journal of Electromagnetic Waves and Applications*, vol. 32, no. 13, pp. 1629-1643, 2018.
- [34] A. Dastranj and F. Bahmanzadeh, "A compact UWB antenna design using rounded inverted L-shaped slots and beveled asymmetrical patch," *Progress In Electromagnetics Research C*, vol. 80, pp. 131-140, 2018.
- [35] A. Dastranj and F. Bahmanzadeh, "Ground plane effect suppression method to design a low-profile printed UWB antenna," *Progress In Electromagnetics Research M*, vol. 88, 91-100, 2020.
- [36] A. Dastranj and M. Bornapour, "UWB planar conical horn-shaped self-complementary bow-tie antenna," *Journal of Communication Engineering (JCE)*, vol. 8, no 1, pp. 20-33, winter and spring 2019.
- [37] A. Dastranj and Z. Javidi, "A Multi-Band Asymmetric Stepped-Slot Antenna for DCS, PCS, WiMAX, 4G, and WLAN Applications," *Journal of Communication Engineering (JCE)*, vol. 8, no 1, pp. 9-20, January-June 2020.
- [38] Shaza El-Nady, Hany Mahmoud Zamel, Moataza Hindy, Abdelhalim A. Zekry and Ahmed Attiya, "Gain Enhancement of a Millimeter Wave Antipodal Vivaldi Antenna by Epsilon Near-Zero Metamaterial," *Progress In Electromagnetics Research C*, vol. 85, pp. 105-116, 2018.
- [39] S. T. Van, G. Kwon and K. C. Hwang, "Planer super - wideband loop antenna with asymmetric coplanar strip feed," *Electronics Letters*, vol. 52, no. 2, pp. 96 –98, 2016.
- [40] J. Liu, K.P. Esselle, S.G. Hay and S.S. Zhong, "Compact super-wideband asymmetric monopole antenna with dual -branch feed for bandwidth enhancement," *Electronics Letters*, vol. 49, no. 8, April 2013.
- [41] A. Singhal, "Octagonal Sierpinski band-notched super-wideband antenna with defected ground structure and symmetrical feeding," *J. Comput Electron*, vol. 17, pp. 1071–1081, 2018.